Radiophysics and Quantum, Electronics, Vol. 43, No. 6, 2000

STUDY OF ATMOSPHERIC-TURBULENCE EFFECTS ON THE FORMATION OF A THERMAL FILM IN THE NEAR-SURFACE WATER LAYER AND THE DYNAMICS OF AIR-WATER HEAT EXCHANGE USING MEASUREMENTS OF THERMAL RADIO EMISSION

K. P. Gaikovich

UDC 621.371:526.2+551.526+528.811+551.501

On the basis of radiometric measurements of thermal radio emission from water at wavelengths 2.3 and 5 mm. we study the dynamics of heat and mass transfer through a water-air boundary, which is related to atmospheric turbulence, and reconstruct the behavior of the water-temperature profile and the heat flux through this boundary. The heat-flux components due to evaporation and thermal conductivity and the evaporation rate from unit surface are determined. Turbulence-induced variations in the depth of the atmospheric viscous sublayer are studied. Statistical parameters of the water-surface temperature variations are calculated. We find that these variations were much greater than the turbulent fluctuations of the air temperature under the measurement conditions.

1. INTRODUCTION

In a number of papers [1-6], a theory of radio-thermal sounding was developed. It is based on the joint solution of the thermal conductivity equation and the radiation transfer equation for radio emission. The obtained relations allow one to determine the evolution of the temperature profile in a medium and of heat flux through a halfspace boundary using single-wavelength measurements of the dynamics of brightness temperature of thermal radio emission of this halfspace at a given direction. These formulas were applied successfully in [5,6] to analyze thermal regimes of the soil and the boundary atmospheric layer using, respectively, the cm-wave emission from the soil and the dynamics of atmospheric emission in the center of the oxygen absorption line at a wavelength of 5 mm [5, 6]. The capabilities of the radiometry of water were first analyzed under laboratory conditions using multi-wavelength methods. In particular, reconstruction of the stationary in-depth temperature profile of bulk water was performed in [3, 7], and the dynamics of the temperature profile in the course of internal-wave propagation was determined in [8]. In these papers, a temperature profile was reconstructed by solving an ill-posed integral Fredholm equation of the 1st kind for the brightness temperature using the Tikhonov method. In principle, the same approach can be used to study the dynamics of the temperature regime in the case of nonstationary boundary conditions. However, from the point of view of problem solving, the single-wavelength technique mentioned above is well posed, and the calibration and formulation of the antenna package of the corresponding radiometric system are not only drastically simpler but also potentially promising for application under natural conditions. Therefore, radiometric measurements of the temporal profile of thermal radio emission from bulk water at wavelength 5 mm were used in laboratory studies [9, 10] of the capabilities of radiometric monitoring of heat- and mass-transfer dynamics on the water-air boundary. The following results of these studies can be pointed out. The dynamics of water- and air-temperature profiles and the heat flux through the interface, which

Institute of the Physics of Microstructures of the Russian Academy of Sciences, Nizhny Novgorod, Russia.Translated from Izvestiya Vysshikh Uchebnykh Zavedenii, Radiofizika, Vol. 43, No. 6, pp. 520-529, June, 2000. Original article submitted December 16, 1999.

is caused by artificial turbulization of the air above the water surface, were reconstructed. The heat-flux components due to evaporation and heat exchange were distinguished, and the evaporation rate from unit surface was determined. An equation was obtained which allows one to find the viscous-sublayer depth in the air using the value of the heat flux, and the dynamics of the depth of this layer under the experimental conditions was reconstructed. An accuracy of 0.07 K of the temperature-profile reconstruction was found by comparison to the results of direct measurements. The effect of convection (development of thermics in the cooled boundary layer) and water turbulence on the dynamics of thermal emission and accuracy of its interpretation was studied.

Studies of the thermal regime of a boundary water layer of thickness of a few centimeters are quite topical due to the fact that the temperature gradient in this layer determines the heat exchange between the ocean and atmosphere, while the use of contact methods is hampered and disturbs the parameters of the medium studied, especially in the case where fast processes are monitored [11].

The approach developed in [9, 10] was implemented in open-air experiments in which the heat-exchange dynamics was determined by the natural atmospheric turbulence [12]. The results obtained on the basis of the analysis of these measurements at wavelengths 2.3 and 5 mm are reported in this paper.

We should also mention the laboratory [13] and marine [14] studies of the effect of the thermal film on radiometric measurements at a wavelength of 5 mm. In [13], as well as in our papers [9,10], the dynamics of water brightness temperature in a small cell was studied in the course of cooling in contact with ambient air of a temperature much lower that the water temperature, the temperature difference between air and water being about 5—10 K.

2. RADIOMETRIC MEASUREMENTS

Emission from the water [12] was measured using a facility comprising a water cell of 2x1.5x0.2 m in size, 2.3- and 5-mm radiometers, and contact water-temperature sensors. The nominal sensitivity of the radiometers was equal to 0.03 — 0.05 . The scalar-horn antennas located at a height of 1 m above the water surface had a pattern width of about 5°, so that the angular-pattern spot on the water surface was about 10 cm in diameter. The cell size chosen ensured that the studied object is sufficiently homogeneous over the angular-pattern spot and the depth of the viscous sublayer is small compared to the system dimensions. The latter is necessary so that the horizontal heat and water-vapor transfer through the cell edges compared to the vertical diffusion in the sublayer can be neglected. The measurements of brightness temperature T_b were calibrated using the water being measured at temperatures different by about 10 K. A homogeneous temperature distribution in the cell was achieved by mixing. The measurements were performed under a reflecting screen, which ensured a constant and homogeneous level of the background radiation temperature, which was close to the brightness temperature of the water. The use of the screen allowed us to almost completely compensate for the reflection coefficient R from water, while the calibration technique, in which the reference brightness temperature is put equal to the water temperature, makes the condition $R = 0$ valid [9, 10]. As a result, the measured value of T_b was equal to the thermometer readings with an accuracy comparable to the fluctuation sensitivity of the radiometer.

Thermal radio emission at wavelengths of 5 and 2.3 mm is formed in a skin layer of depth of about 0.15 and 0.1 mm, respectively. In the case of high temperature gradients observed in thermal films, the temperature differs from the surface value by about 0.3, which exceeds the obtained sensitivity of the measurements. Therefore, one cannot put the brightness temperature equal to the surface one. Measurements at 5 mm are much more suitable for the water radiometry since this wavelength corresponds to the center of a strong absorption band of oxygen molecule, in which the background radio brightness temperature is close to the ambient air temperature. The background atmospheric emission is formed in a layer of about 250 m in depth, and variations in this background are not larger than the background temperature fluctuations. The background radiation at 2.3 mm is strongly influenced by clouds. In this case, calibration and measurement conditions are subject to much more stringent constraints. As a result, the wavelength of 2.3 mm was only used in some experiments for comparison to the measurements at 5 mm. All the measurements

were performed under cloudless weather conditions.

3. DETERMINATION OF THE HEAT-EXCHANGE DYNAMICS BETWEEN WATER AND AIR DUE TO THE EFFECT OF ATMOSPHERIC TURBULENCE

This work is aimed at the analysis of the dynamics of the thermal regime of the surface water layer, which is formed under the action of natural air turbulence in the vicinity of its boundary. Initially, water in the cell was in fairly stable thermal equilibrium with the atmosphere, which was formed by solar heating, balance of emitted and absorbed thermal radiation, evaporation, and heat conduction. Next, a homogeneous temperature distribution was created by water mixing, solar emission was screened, and the process of water cooling due to evaporation and heat exchange with ambient air was observed. In this case, the radiative heat exchange at small temperatures between water and screen is eliminated almost completely by screening, so turbulent, variations in the ambient air flowing over the surface play the dominant role. This case is somehow similar to the cooling of a stagnant pool, which is related to the appearance of clouds.

Variations in the velocity of turbulent air motion give rise to strong fluctuations of the depth of the viscous sublayer above the water surface. In this case, we treat the viscous sublayer in the hydrodynamical, rather than statistical, sense, i.e., the turbulence is assumed to change permanently the depth of this layer. The flow in the viscous sublayer becomes laminar, and transfer of heat and water vapor (small constituent) begins due to a molecular-diffusion mechanism. Note that, in the framework of the statistical approach, the turbulent-diffusion coefficient in the viscous sublayer is assumed to decrease down to the surface value of the molecular-diffusion coefficient. Transfer processes in the viscous sublayer are determined by temperature and water-vapor gradients in the region between the water surface and the upper boundary of the viscous sublayer. Above this boundary, a turbulence-diffusion regime is realized, which is characterized by a diffusion coefficient much greater than the corresponding coefficient in the viscous sublayer. This allows one to assume that it is in the viscous sublayer where the entire variation in the temperature and density of water vapor from the values of these quantities near the water surface to the corresponding values in the ambient air takes place. Thus, the model of the ambient air near the water surface is two-layer.

Since the size of the angular-pattern spot exceeds the inner scale of turbulence and the integration time is longer than the period of the fastest fluctuations, the domain of influence of spatial and temporal spectra of the atmospheric turbulence should be limited from the high-frequency side. Nevertheless, the results of laboratory studies [9, 10] based on the comparison of reconstructed dynamics and the data of direct measurements reveal that such an approach allows one to describe the heat exchange with a high degree of accuracy. This is explained by the fact that fast fluctuations of periods less than the integration time are smoothed by the inertial process of water heating.

Strong variations in the water-vapor concentration in the viscous sublayer, which are proportional to the variations in the depth of this layer induced by the atmospheric turbulence, result in variations in the water-vapor flux (evaporation) and, therefore, in the corresponding variations in the heat flux related to evaporation. The same is true for the temperature gradient in the viscous sublayer whose variations stipulate the dynamics of the thermal-conductivity heat flux. As a result, the surface layer of water is cooled quickly, and the corresponding dynamics of the brightness temperature of its thermal radio emission is detected by sensitive radiometers. The subsequent analysis allow one to reconstruct in detail the heat and mass transfer through the air-water boundary.

The measured temporal dependence of the radio brightness temperature $T_b(t)$ was used to reconstruct the subsurface temperature profile $T(z, t)$ in the halfspace $z < 0$ with homogeneous temperature conductivity a^2 and absorption coefficient γ of thermal radiation. This was done using the formula obtained from joint solution of heat-conductivity and radiation-transfer equations [4-6]:

$$T(z,t) = \int_{-\infty}^{t} T_b(\tau)\,(-z)\exp\left[-\frac{z^2}{4a^2\,(t-\tau)}\right]\frac{\mathrm{d}\tau}{\sqrt{4\pi a^2\,(t-\tau)^3}} +$$

$$+\frac{1}{\gamma a}\int\limits_{-\infty}^{t} T_{\mathrm{b}}'(\tau)\exp\left[-\frac{z^2}{4a^2\,(t-\tau)}\right]\frac{\mathrm{d}\tau}{\sqrt{\pi\,(t-\tau)}}\,. \tag{1}$$

The integral in the second term of Eq. (1) can be evaluated by parts at $z < 0$:

$$T(z,t)=\int\limits_{-\infty}^{t} T_{\mathrm{b}}(\tau)\exp\left[-\frac{z^2}{4a^2\,(t-\tau)}\right]\left[\frac{1}{\gamma}\left(\frac{z^2}{2a^2\,(t-\tau)}-1\right)-z\right]\frac{\mathrm{d}\tau}{\sqrt{4\pi a^2\,(t-\tau)^3}}\,. \tag{2}$$

Equation (2) fails to describe the surface temperature at $z = 0$ where the following formula should be used:

$$T_0(t)=T_{\mathrm{b}}(t)+\frac{1}{\gamma a}\int\limits_{-\infty}^{t} T_{\mathrm{b}}'\frac{\mathrm{d}\tau}{\sqrt{\pi\,(t-\tau)}}=T_{\mathrm{b}}(t)+\frac{1}{2\gamma a}\int\limits_{-\infty}^{t}[T_{\mathrm{b}}(t)-T_{\mathrm{b}}(\tau)]\frac{\mathrm{d}\tau}{\sqrt{\pi\,(t-\tau)^3}}\,. \tag{3}$$

The heat flux through the interface is determined by the time derivative of brightness temperature [4-6]:

$$J(t)=-\frac{k}{a^2\gamma}\left[T_{\mathrm{b}}'(t)+\gamma a\int\limits_{-\infty}^{t} T_{\mathrm{b}}'(\tau)\frac{\mathrm{d}\tau}{\sqrt{\pi\,(t-\tau)}}\right], \tag{4}$$

where k is the heat-conductivity coefficient.

In the framework of the model considered, the heat flux $J(t)$ can be presented as the sum of the flux due to evaporation and the following flux due to molecular heat conduction in the viscous sublayer:

$$J(t)=J_q(t)+J_T(t)=-r\rho D_q\left.\frac{\mathrm{d}q}{\mathrm{d}z}\right|_{z=0}-k\left.\frac{\mathrm{d}T}{\mathrm{d}z}\right|_{z=0}=-r\rho D_q\frac{q_{\mathrm{a}}-q(0)}{d}-\rho c_p a^2\frac{T_{\mathrm{a}}-T(0)}{d}\,, \tag{5}$$

where q is the number density (specific humidity) of water vapor treated as a minor constituent, r is the specific evaporation heat, ρ is the air density, D_{q} is the diffusion coefficient of water vapor, c_{p} is the specific heat capacity of air at constant pressure, d is the depth of the viscous sublayer, and q_{a} and T_{a} are, respectively, the number density and temperature in the turbulent air layer above the viscous sublayer. The air density $\rho = P/(R_{\mathrm{a}}T)$, where P is the pressure and R_{a} is the gas constant of the air.

According to the estimates, linear profiles of temperature and water-vapor density in a viscous sublayer of thickness 2 mm are formed during a characteristic time of about 0.2 s, so that the gradients of temperature and water-vapor density in this layer can be assumed constant. According to the evaporation theory, the number density $q(0)$ of water vapor near the surface in the case of vapor removal is different from the saturated number density q_{s} determined by the temperature of air-water interface, but the former quantity can be expressed in terms of the latter one. Thus, all the parameters in Eq. (5) are entirely determined by the dynamics of the water-surface temperature. It is shown in [9, 10] that Eq. (5) can be reduced to a quadratic equation with respect to the viscous-sublayer depth. Note that both roots of this equation are physically meaningful, but the case corresponding to the maximum root is realized under the usual atmospheric conditions.

We should note that the method described is adequate as long as the heat-conductivity equation, used to derive the initial formulas, remains valid. In [9, 10], the effect of convection and turbulence in water on the dynamics of thermal emission and interpretation of measurements was analyzed. In particular, the Rayleigh number, determining the stability of temperature stratification in a cool film, reaches its critical value due to strong evaporation from the water surface, and then convective motion (descent of a thermic) develops. In the experiments described, the Rayleigh number, checked continuously using the reconstructed temperature profile, did not exceeded the critical value, and convection was not developed.

Figure 1 shows an example of the measured dynamics of the brightness temperature at wavelength 5 mm and the water-temperature profiles at different depths reconstructed using this dynamics. The result of temperature reconstruction is shown in more detail in Fig. 2.

The measurements were performed under conditions corresponding to cloudless weather and weak wind which occasionally fell to calm. During the measurements illustrated by Figs. 1 and 2, the wind changed as follows: the wind velocity was about constant at a level of 5 —7 m/s during the time from 0 to 50 s; the wind fell to calm from 50 to 90 s; very weak wind with velocity of about 0 — 3 m/s was observed from 90 to 160 s; the wind fell to calm from 160 to 190 s; the wind velocity was about 5 — 7 m/s from 190 to 200 *s:* and weak wind with velocity of about 3 m/s was observed from 200 to 250 s.

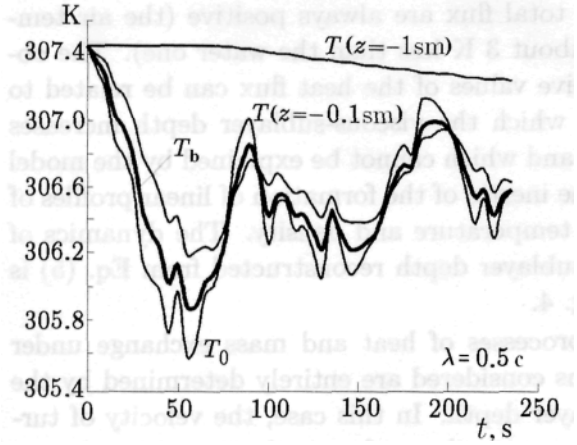

Fig. 1. The dynamics of brightness temperature Tb at wavelength 5 mm and the dependences of the water temperature near the surface, reconstructed using Eq. (3), and at depths 1 mm and 1 cm, reconstructed using Eq. (2).

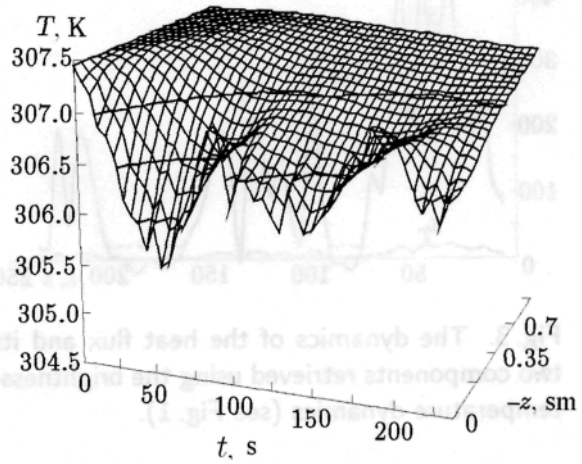

Fig. 2. The dynamics of the temperature profile of a cool thermal film, reconstructed using the measured dynamics of the brightness temperature (see Fig. 1).

It is seen from Figs. 1 and 2 that sharp variations in the water-surface temperature are transferred, with a greater delay, to deeper layers where these variations are gradually smoothed and eventually become a smooth temperature decrease. Corresponding dynamics of the heat flux through the water-air interface, determined from Eq. (4), is shown in Fig. 3.

These results reveal that the heat flux undergoes very strong and fast variations. Using Eq. (5), one can determine the dynamics of the viscous-sublayer depth and then calculate the components of the total heat flux, which are related to evaporation and heat exchange. These components are shown in Fig. 3, as well. It is seen that the dominant role is played by evaporation. During the first 60 seconds, the flux J reached the values obtained in laboratory experiments in which a fan was used to create an air blow along the surface [9, 10]. Then, however, the air turbulence rapidly decreased, and the resulting temperature gradient in the formed film was insufficient for the Rayleigh number to exceed the critical value and a convective thermic to develop.

The accuracy of the above-described method for reconstructing heat-flux dynamics can be estimated on the basis of numerical modeling. It is seen from Eq. (4) that the method is not sensitive to absolute measurement errors of brightness temperatures. Assuming that the random noise is uncorrelated over the integration time, we find that the realized sensitivity of 0.03 K implies a mean error of heat-flux determination of about 15%. Maximum values of the heat flux observed in the experiments correspond to a temperature difference of about 0.7 K in a film of thickness 1 mm in the case of a linear profile. This is quite a realistic estimate as far as the known parameters of thermal films are concerned [11]. The data in Fig. 3 are also in agreement with the measurements [13] in which the mean heat flux was determined using water cooling in a cell. The absence of an alternative method for measurement of fast heat-flux variations is

an important advantage of the method developed, but it is difficult to confirm the obtained results by independent measurements. It was proposed in the literature (see, e.g., [13]) that the heat flux can be estimated using the difference in water brightness temperatures measured at two different frequencies (e.g., at 60 GHz and in the IR band). We should note that, in addition to errors due to nonlinearity of the temperature profile, such a method will be quite sensitive to the matching accuracy of the measurements in different channels. For example, a mismatch of 0.1 K, which is quite difficult to achieve taking all the factors into account, gives rise to an error of about 300 W/m^2 in the determination of the heat-flux value.

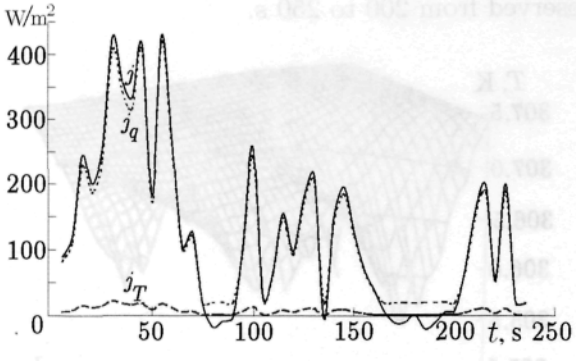

Fig. 3. The dynamics of the heat flux and its two components retrieved using the brightness-temperature dynamics (see Fig. 1).

Changes in sign of the heat flux observed at the 75th and after 150th second cannot be explained in the framework of the model considered, since both components of the total flux are always positive (the air temperature is about 3 K less than the water one). The obtained negative values of the heat flux can be related to the cases in which the viscous-sublayer depth increases significantly and which cannot be explained by the model neglecting the inertia of the formation of linear profiles of water-vapor temperature and density. The dynamics of the viscous-sublayer depth reconstructed from Eq. (5) is shown in Fig. 4.

The processes of heat and mass exchange under the conditions considered are entirely determined by the viscous-sublayer depth. In this case, the velocity of turbulent air blow over the surface is the actual key factor, since this velocity determines the sublayer depth. Generally, the viscous-sublayer depth under weak-wind of calm conditions turned out to be greater than the value of 2 mm obtained in the laboratory experiment [9,10] using an air blower. The values in excess of 4 mm, corresponding to calming wind, are not shown in Fig. 4, since, as was pointed out earlier, the time of linear-profile formation in the viscous sublayer should not be neglected when analyzing this case.

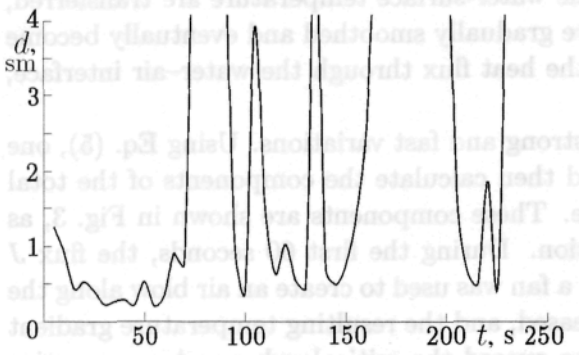

Fig. 4. Variations in the viscous-sublayer depth in the air, determined using the brightness-temperature dynamics (see Fig. 1).

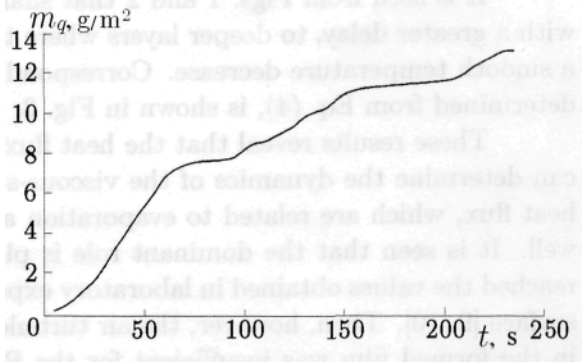

Fig. 5. Evaporation from unit surface under the action of atmospheric turbulence.

Integrating the heat-flux component related to evaporation and normalizing it to the specific evaporation heat [9, 10], one can easily determine the dynamics of evaporation from unit surface:

$$m_q(t) = \frac{1}{r}\int_0^t J_q(t')\,\mathrm{d}t'. \qquad (6)$$

Corresponding results are presented in Fig. 5.

4. COMPARISON OF THE RESULTS OF MEASUREMENTS AT TWO WAVELENGTHS

As was already mentioned above, the measurements at wavelength 2.3 mm were performed mainly for comparison with the results obtained at wavelength 5 mm. The brightness-temperature dynamics at 2.3 and 5 mm during a short time interval is presented in Fig. 6. Also shown in this figure are the results of reconstruction of the surface temperature and the temperature at a depth of 1 mm using the data corresponding to each wavelength.

It is seen from Fig. 6 that the discrepancy of the reconstructed temperature profiles is not larger than the reconstruction error determined in [9, 10]. The reconstruction error of the surface temperature was not determined earlier experimentally or theoretically, since the derivative over the experimental data enters Eq. (3) for surface-temperature reconstruction, while it is difficult to measure this value directly and compare it with the reconstruction results. Therefore, the dependences presented in Fig. 6 allow one to obtain a reasonable estimate of 0.1 — 0.2 K for such an error.

Measurements at two wavelengths are of independent interest, since the following formula, relating the dynamics of brightness temperatures T_{b1} and T_{b2} of a medium at two wavelengths λ_1 and λ_2, respectively, was obtained in [15, 16]:

$$T_{b2}(t) = \frac{\gamma_2}{\gamma_1} T_{b1}(t) + \int_{-\infty}^{t} T_{b1}(\tau) \left(1 - \frac{\gamma_2}{\gamma_1}\right) \gamma_2 a \left[\frac{1}{\sqrt{\pi\,(t-\tau)}} - \gamma_2 a\, e^{(\gamma_2 a)^2 (t-\tau)} \operatorname{erfc}(\gamma_2 a \sqrt{t-\tau})\right] d\tau. \quad (7)$$

Here γ_1 and γ_2 are, respectively, the absorption coefficients of radiation at each wavelength. Figure 7 shows the measurement data on the dynamics of brightness temperatures at $\lambda_1 = 2.3$ and $\lambda_2 = 5$ mm and the results of their mutual calculation using Eq.(7).

It is seen that dynamics of the brightness temperature at wavelength 2.3 mm calculated using the measurements at 5 mm and vice versa are in good agreement.

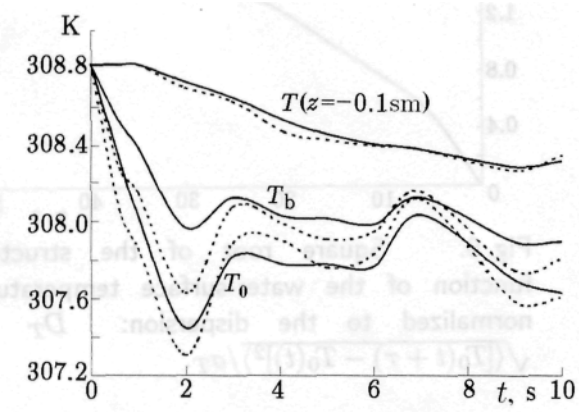

Fig. 6. The dynamics of brightness temperatures measured at wavelengths of 2.3 (dashed line) and 5 mm (solid line) and the results of reconstruction of the temperatures on the surface and at a depth of 1 mm using the data at each wavelength.

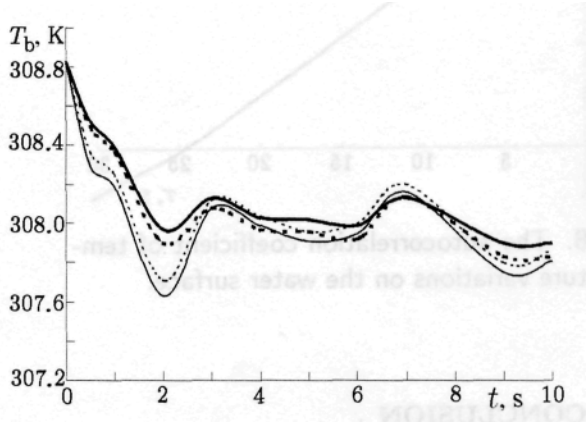

Fig. 7. The measured dynamics of brightness temperatures measured at wavelengths 2.3 and 5 mm (thick and thin solid line, respectively) and the results of their mutual calculation using Eq. (7): the thick dashed line corresponds to T_{b2} calculated using T_{b1}, while the thin dashed line, to T_{b1} calculated using T_{b2}.

5. STATISTICAL ANALYSIS OF TEMPERATURE VARIATIONS OF WATER SURFACE

It is of interest to study the statistical properties of variations in the water-surface temperature. In Fig. 8, we present the results of calculation of the autocorrelation coefficient $R_T(\tau)$.

The square root of the structure function of the water-surface temperature, normalized to the r.m.s. variation σ_T = 0.44 K, is plotted in Fig. 9. If Taylor's model of "frozen turbulence" is applied, the temporal correlation function in Fig. 8 and the structural correlation function in Fig. 9 can be considered as the corresponding spatial functions of the argument $\rho = V\tau$, where V is the mean wind velocity in the boundary layer. The time of correlation loss in Fig. 8 is about the time of transfer of an external turbulence scale of about 100 m by a wind of velocity about 5 m/s.

The results show that the r.m.s. difference in water-surface temperatures measured at two different time instants increases with increasing time difference. If $\tau > 25$ s, this value exceeds 1 K which is much greater than the air-temperature fluctuations amounting to 0.05 K during the specified time interval (the latter value is obtained using radiometric data on the proper thermal emission of the atmosphere at wavelength 5 mm). Evidently, this effect is related to the dominant influence of the evaporation rate on the water-surface temperature variations, as compared to the corresponding effect of thermal-conduction heat exchange between water and air.

It is interesting to note that the characteristic correlation time of water-surface temperature variations is approximately equal to the time of formation of a cooled thermal film in a turbulent water, which is about 10 s according to the experiment [9, 10]. Thus, one can conclude that a cooled thermal film, formed due to the influence of atmospheric turbulence under similar conditions and subject to waves or flows generating turbulence in the surface layer of water, should undergo more or less strong variations resulting in the corresponding spatial irregularity of the film structure. These variations depend on the air humidity and the temperature difference between water and air. They should decrease if the air humidity reaches the saturation value and the air temperature becomes close to the water one.

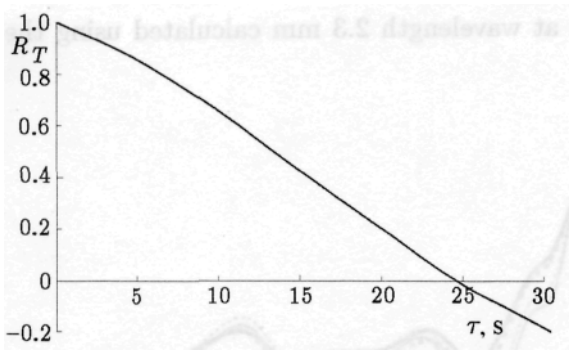

Fig. 8. The autocorrelation coefficient of temperature variations on the water surface.

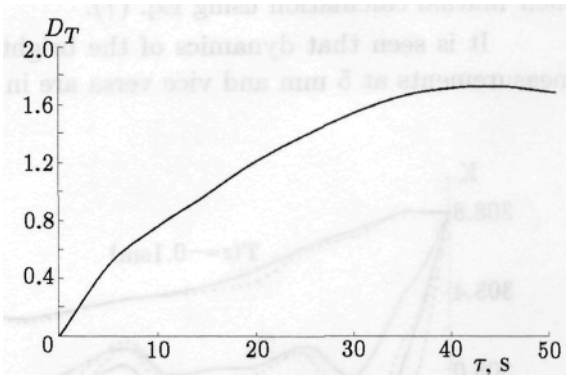

Fig. 9. Square root of the structure function of the water-surface temperature, normalized to the dispersion:

$$D_T = \sqrt{<[T_0(t+\tau) - T_0(t)]^2>} / \sigma_T .$$

6. CONCLUSION

The main result of this paper is the following. For the first time, using the dynamics of thermal radio emission, we were able to obtain new physical information on the heat and mass exchange between the water surface and atmosphere. We reconstruct the dynamics of the temperature profile in a surface layer of water subject to atmospheric turbulence under weak-wind blowing conditions under which a cooled thermal film is formed during a time of about 10 s. Fast variations in the heat flux through the interface, as well as its main components related to evaporation and heat conduction, are reconstructed. Our analysis shows that the viscous-sublayer depth is subject to strong wind-induced variations. The latter determined

its regulating role in the heat-exchange process, since the heat-flux and water-evaporation components are inversely proportional to the sublayer depth. We studied the statistical characteristics, such as correlation coefficient and structure function, of the water-surface temperature and find that the variations of the water-surface temperature, observed in our experiment, are about an order of magnitude greater than the temperature fluctuations of ambient air.

Our results show that the radiometric method is applicable to studies of the dynamics of heat exchange between the atmosphere and water surface and can yield important physical data on the behavior of this process in various natural conditions (in fresh and salty water, at different ratios of water and air temperatures, and at different values of the air humidity). Analysis of the spatial structure of the heat exchange, in particular, the spatial variability of the viscous-sublayer depth, is the most interesting. The depth of the viscous sublayer may probably undergo drastic changes at scales of a few tens of meters or even less. This gives evidence of the strong irregularity of the heat and water-vapor fluxes from the water surface to the atmosphere, which in turn should affect the atmospheric turbulence and convection.

Similar studies of the dynamics of thermal emission from different kinds of soil can also yield interesting results on the features of their energy exchange with the atmosphere.

The author is grateful to A. V. Troitsky for help in performing the experiments.

This work was supported by the Russian Foundation for basics Research (project No. 96-02-16514).

REFERENCES

1 . K. P. Gaikovich and A.N.Reznik, *Izv. Vyssh. Uchebn. Zaved., Radiofiz.,* 33, No. 11, 1343 (1989).

2. K. P. Gaikovich, *Issled. Zemli iz Kosmosa,* No. 6, 71 (1990).

3. K. P. Gaikovich, A.N. Reznik, and R. V. Troitsky, in: *llth Annual Int. Symp. Geosci. Remote Sensing (IGARSS-91). Helsinki, Finland, 1991, 3,* 1(195) (1991).

4. K. P. Gaikovich, *Izv. Vyssh. Uchebn. Zaved., Radiofiz.,* 36, No. 1, 16 (1993).

5. K. P. Gaikovich, *Izv. Vyssh. Uchebn. Zaved., Radiofiz.,* 36, No. 10, 912 (1993).

6. K. P. Gaikovich, *IEEE Trans. Geosci. Remote Sensing,* 32, No. 4, 885 (1994).

7. K. P. Gaikovich, et.al., *Izv. Akad. Nauk SSSR, Ser. Fiz. Atmos. Okeana,* 23, No. 7, 761 (1987).

8. K. P. Gaikovich, A.N.Reznik, and R. V. Troitsky, *Izv. Vyssh. Uchebn. Zaved., Radiofiz.,* 36, No. 3-4, 216 (1993).

9. K. P. Gaikovich and R.V. Troitsky, *Izv. Vyssh. Uchebn. Zaved., Radiofiz.,* 40, No. 3, 351 (1997).

10. K. P. Gaikovich and R.V. Troitsky, *IEEE Trans. Geosci. Remote Sensing,* 36, No. 1, 341 (1998).

1 1 . K.N.Fedorov and A. I. Ginzburg, *Subsurface Layer of the Ocean* [in Russian] Gidrometeoizc at, Leningrad (1988).

12. K. P. Gaikovich and R. V.. Troitsky, in: *Proc. Third Int. Kharkov Symp. "Physics and Engineering of Millimeter and Submillimeter Waves" MSMW'98. Kharkov, Ukraine, Sept. 15-17, 1998,* Inst. Radio-phys. Electronics, Kharkov (1998), Vol.2, p. 509.

13. Yu. G. Trokhimovski, et.al., *Issled. Zemli iz Kosmosa,* No. 5, 3 (1998).

14. Yu.G. Trokhimovski, et.al., *IEEE Trans. Geosci. Remote Sensing,* 36, No. 1, 3 (1998).

15. K. P. Gaikovich, *IEEE Trans. Geosci. Remote Sensing,* 34, No. 2, 582 (1996).

16. K. P. Gaikovich, *Izv. Vyssh. Uchebn. Zaved., Radiofiz.,* 39, No. 4, 399 (1996).